Journal of Biotechnology 192 (2014) 11–19

Contents lists available at ScienceDirect

Journal of Biotechnology

journal homepage: www.elsevier.com/locate/jbiotec

Development of an ELP-Z based mAb affinity precipitation process using scaled-down filtration techniques

Rahul D. Sheth[a,b], Bharat V. Bhut[b], Mi Jin[b], Zhengjian Li[b], Wilfred Chen[c], Steven M. Cramer[a,*]

[a] Department of Chemical and Biological Engineering, Center for Biotechnology and Interdisciplinary Studies, Rensselaer Polytechnic Institute, 110 8th Street, Troy, NY 12180, United States
[b] Biologics Process Development, Bristol-Myers Squibb, East Syracuse, NY, United States
[c] Department of Chemical and Biomolecular Engineering, University of Delaware, Newark, DE, United States

ARTICLE INFO

Article history:
Received 3 July 2014
Received in revised form
20 September 2014
Accepted 24 September 2014
Available online 5 October 2014

Keywords:
Elastin-like polypeptides
Monoclonal antibodies
Affinity precipitation
Tangential flow filtration
Normal flow filtration
Scale-up

ABSTRACT

In this work, a proof of concept elastin-like polypeptide-Z domain fusion (ELP-Z) based monoclonal antibody (mAb) affinity precipitation process is developed using scaled-down filtration techniques. Tangential flow filtration (TFF) is examined for the recovery of ELP-Z-mAb precipitates formed during the mAb binding step and the ELP-Z precipitates formed during the mAb elution step. TFF results in complete precipitate recovery during both stages of the process and high host cell protein and DNA impurity clearance after diafiltration. Total recycle TFF experiments are then employed to determine permeate flux as a function of the precipitate concentration for both stages of the process. While the ELP-Z-mAb precipitate recovery step resulted in high permeate flux (550–600 L/m^2/h/bar), the ELP-Z precipitates are shown to severely foul the TFF membrane, causing rapid flux decay. Confocal microscopy of the ELP-Z-mAb and ELP-Z precipitates suggests significant differences in the morphology and the kinetics of formation of these precipitates, which is likely responsible for their different behavior during TFF. Finally, an alternative normal flow filtration strategy is developed for the ELP-Z precipitate recovery step during mAb elution, using a combination of 5 μm and a 0.45/0.2 μm filters. Using this approach, the ELP-Z precipitates are separated from the final mAb elution pool at high volumetric throughputs and high ELP-Z recovery (96%) is obtained after resolubilization from the filter. This study demonstrates that the ELP-Z affinity precipitation process can be readily scaled up using conventional membrane processing.

1. Introduction

Protein A chromatography is ubiquitous to the monoclonal antibody industry (Fassina, 2001; Hober et al., 2007; Huse et al., 2002). However, relatively high resin costs and slow volumetric throughputs for this step are often an impediment for dealing with increasingly higher upstream mAb titers. Affinity precipitation, on the other hand, may offer advantages as a mAb capture step in terms of scalability and processing simplicity at reduced costs (Hilbrig and Freitag, 2003).

A reversible and tunable phase transition property, modularity of sequence design and the ease of production have made elastin-like polypeptides (ELPs) an attractive tool for protein purification (Banki et al., 2005; Ge et al., 2005; Kim et al., 2005; Meyer and Chilkoti, 1999; Stiborova et al., 2003; Sun et al., 2005). ELPs consist of elastin-based pentapeptide repeating motifs (VPGXG), where X is the guest amino acid residue. ELPs can reversibly self associate above a critical inverse transition temperature (T_t) (Urry, 1997) and this property can be altered by changing the ELP design and/or the solution conditions (Cho et al., 2008; Meyer and Chilkoti, 2004).

Kim et al. (2005) have previously employed an ELP-Protein A fusion for the purification of mAbs via affinity precipitation. This approach enables the ELP-Protein A fusion to be produced independently of the mAb thus not affecting mAb production and titers. Protein A (42 kDa) was later replaced by the Z domain (6.6 kDa) allowing for higher elastin-like polypeptide-Z domain fusion (ELP-Z) (39.4 kDa) production yield (Madan et al., 2013). Further, a High-Throughput Screening (HTS) protocol has been developed to rapidly identify optimal operating conditions for an ELP-Z based affinity precipitation process (Sheth et al., 2013). Finally, recent studies in our group with industrial mAb harvest feed have shown that an ELP-Z based affinity precipitation process can result in high

* Corresponding author at: Department of Chemical and Biological Engineering, Center for Biotechnology and Interdisciplinary Studies, Rensselaer Polytechnic Institute, 110 8th Street, Troy, NY 12180-3590, United States. Tel.: +1 518 276 6198; fax: +1 518 276 4030.
E-mail address: crames@rpi.edu (S.M. Cramer).

http://dx.doi.org/10.1016/j.jbiotec.2014.09.020
0168-1656/

levels of host cell protein (HCP) and DNA impurity clearance while maintaining high mAb yields (Sheth et al., 2014). While the bench scale performance of the affinity precipitation process has been promising, scalability of the process is also critical in determining its bioprocessing potential.

Continuous centrifugation and membrane filtration have been widely employed for precipitate recovery in a biomanufacturing setting. Continuous centrifugation is commonly performed using disk stack or multichamber bowl centrifuges (Boychyn et al., 2004). Precipitate recovery during continuous centrifugation is governed by the particle size distributions (PSDs) and density of the precipitates. During continuous centrifugation, it is common for the process feeds to encounter high flow stresses at the feed zone (Boychyn et al., 2001), which can break shear sensitive particles, such as protein precipitates (Hoare et al., 1982), thus affecting their clarification efficiency (Neal et al., 2003). In addition, the high shear rates may also produce local heating effects which can adversely affect product quality.

Membrane filtration on the other hand, can be performed using the desired pore size membranes to achieve high levels of precipitate recovery. However, concentration polarization and membrane fouling due to cake formation and/or pore blockage can often reduce the volumetric throughputs attainable during filtration (Belfort et al., 1994). Membrane filtration can be performed in either the tangential flow mode or the normal flow/dead-end mode. While tangential flow filtration (TFF) results in high volumetric throughputs due to reduced membrane fouling, it often requires large diafiltration volumes for the complete recovery of soluble product or the removal of soluble impurities which can result in product dilution. Normal flow filtration (NFF) on the other hand, results in less buffer consumption and product dilutions, but can produce lower volumetric throughputs due to significant concentration polarization and membrane fouling. Thus, the choice of the appropriate mode of operation for a given filtration process must be based on proper consideration of the behavior and composition of the process streams.

Microfiltration membranes have been previously employed for recovery of soy protein precipitates obtained by acid treatment (Bentham et al., 1988; Devereux and Hoare, 1986). NFF and TFF are also commonly used in the food and dairy industry. Venkiteshwaran and coworkers (Venkiteshwaran et al., 2008) have performed detailed studies on the recovery of Immunoglobulin precipitates from bovine serum using scaled-down tangential flow microfiltration. In addition, Chilkoti and coworkers (Ge et al., 2006) have employed syringe and continuous stirred tank based microfiltration for the recovery of ELP-thioredoxin fusion precipitates, suggesting that membrane filtration can be potentially employed for the recovery ELP based precipitates.

In this paper, a proof of concept scaled down membrane microfiltration approach is developed for the recovery of ELP-Z-mAb and ELP-Z precipitates formed during various stages of the mAb affinity precipitation process. TFF is examined for its efficacy to retain ELP-Z-mAb precipitates during the initial mAb binding step and the ELP-Z precipitates during the subsequent mAb elution (dissociation of the ELP-Z-mAb complex) step. While good performance is observed with TFF during the first step, low throughputs are obtained during the ELP-Z precipitate recovery step. Confocal microscopy of the ELP-Z-mAb and ELP-Z precipitates is then carried out to learn more about the nature of these precipitates and to help explain the differences observed during membrane processing. A staged normal flow filtration (NFF) train scheme is then employed for the recovery of the ELP-Z precipitates and the resulting permeate streams are analyzed at each stage for the presence of sieved ELP-Z. Based on these results, a final combination of filters is employed for the recovery of the ELP-Z precipitates using NFF and the process throughputs are determined. This study demonstrates proof of concept for a scalable ELP-Z based mAb affinity precipitation process using membrane filtration techniques and provides insight into the behavior of these systems.

2. Materials and methods

2.1. Materials

A Pellicon XL 50 cm^2, 0.1 μm hydrophilized poly(vinylildene difluoride) (PVDF) cassette was purchased from Millipore (Bedford, MA). 17.3 cm^2 Sartopure PP2 NFF cartridges (5, 1.2, 0.65 and 0.45/0.2 μm) were purchased from Sartorius Stedim (Gottingen, Germany). A Jupiter® 5 μm C4 300A column (4.6 mm × 50 mm) was purchased from Phenomenex (Torrance, CA). A TSK gel G3000SWxl SEC column (7 mm × 300 mm) with accompanying guard column was purchased from Tosoh (Tokyo, Japan). A POROS® A 20 μm column (4.6 mm × 50 mm) and all the SDS PAGE gel supplies were purchased from Life Technologies (Carlsbad, CA). *Escherichia coli* strain BL21(DE3) cells containing the ELP-Z (78 pentapeptide (VPGVG) repeats) plasmid were constructed as described elsewhere (Kim et al., 2005). Bacto tryptone and yeast extract were purchased from BD Biosciences (Franklin lakes, NJ). Glycerol, ampicillin and trifluoroacetic acid (TFA) were purchased from Fisher Scientific (Pittsburgh, PA). CHO HCP ELISA kit, 3G was purchased from Cygnus Technologies (Southport, NC). Sodium hydroxide, potassium phosphate (mono and dibasic), citric acid, sodium phosphate (dibasic), and acetic acid were purchased from JT Baker (Phillipsburg, NJ). Potassium chloride, sodium chloride, acetonitrile (ACN), sodium citrate dihydrate and protease inhibitor cocktail were purchased from Sigma–Aldrich (St. Louis, MO). Sodium sulfate was purchased from EMD Chemicals (Billerica, MA).

2.2. Experimental procedures

2.2.1. ELP-Z expression and purification

The protocol for expression and purification of ELP-Z (39.4 kDa) has been described in detail previously (Sheth et al., 2013). Briefly, *E. coli* strain BL21(DE3) containing the ELP-Z plasmid was grown in Luria Broth (LB) with 100 μg/mL ampicillin at 37 °C and 250 rpm for 16 h. The grown cultures were then sub cultured into Terrific Broth (100 μg/mL ampicillin) and grown for 48 h at 37 °C and 250 rpm. Following cell harvesting and lysis, the inverse phase transition property was employed for the purification of the ELP-Z fusion (Sheth et al., 2013). This protocol typically resulted in ELP-Z production yield of 0.5 g/L media.

2.2.2. Tangential flow filtration (TFF)

2.2.2.1. Processing of the ELP-Z-mAb precipitates. TFF was initially employed for the recovery of the ELP-Z-mAb precipitates on the membrane and the removal of impurities (host cell and media) in the permeate stream. 150 mL of the 3.3 g/L mAb harvest feed was mixed with 60 mL of 8.25 g/L ELP-Z (in PBS) to achieve a 4:1 ELP-Z:mAb molar ratio under constant mixing with a magnetic stir bar at room temperature. ELP-Z-mAb binding was allowed to occur for 5 min followed by the addition of 52.5 mL of 1.25 M Na_2SO_4 (in PBS) to achieve a 0.25 M final concentration to initiate ELP-Z-mAb precipitation. The precipitation was performed in a 500 mL cylindrical glass beaker and the suspensions were mixed using a magnetic stir bar at ~400 RPM. The feed was constantly mixed for 30 min to allow the ELP-Z-mAb precipitates to grow. The precipitate suspension was then added to the TFF system reservoir where it was again constantly mixed for the rest of the experiment. A 50 cm^2 flat sheet 0.1 μm hydrophilized poly(vinylildene difluoride) (PVDF) membrane was employed for the TFF studies (~100 g/m^2 mAb loading). TFF experiments were performed using a AKTAcrossflow (GE Healthcare) system (with ~30 mL system dead volume)

at 1.5 bar trans-membrane pressure (TMP) and a 960 L/m^2/h cross flow rate and the membrane was pre-equilibrated with the precipitation buffer (0.25 M Na_2SO_4 in PBS). The ELP-Z-mAb precipitates were initially concentrated two fold, which was then followed by diafiltration (using the precipitation buffer) using 5 diavolumes for the removal of the soluble impurities in the permeate stream. Finally, the precipitate suspension was concentrated further after the diafiltration.

2.2.2.2. Processing of the ELP-Z precipitates. The ELP-Z-mAb precipitates from the previous step were dissolved by the addition of 50 mM citrate, pH 4 elution buffer to a total volume of 300 mL to allow for mAb elution. The elution pool was then collected in a separate glass beaker and ELP-Z precipitation was initiated by the addition of Na_2SO_4 (in the elution buffer) to a 0.25 M final concentration. The precipitates were again mixed for 30 min. While precipitation of ELP-Z was occurring, the TFF system with filter cassette was cleaned using 0.1 N NaOH, and then pre equilibrated with the precipitation buffer (50 mM citrate, 0.25 M Na_2SO_4, pH 4). The mAb elution pool containing the ELP-Z precipitates was then added to the TFF system reservoir and the same procedure was carried out for the concentration/diafiltration as discussed above. In this case, the eluted mAb was obtained in the permeate stream whereas the ELP-Z precipitates were retained on the membrane. The final mAb elution pool was analyzed for mAb yield and the presence of HCP, DNA and ELP-Z impurities as described in Section 2.3. Finally, the ELP-Z precipitates were re-solubilized in PBS and analyzed.

2.2.2.3. TFF total recycle experiments. For the TFF total recycle experiments for the ELP-Z-mAb precipitate recovery step, the same procedure was followed for the feed preparation as discussed above. At each precipitate concentration, the permeate stream was recycled back into the feed reservoir until a steady state permeate flux was reached and the value was recorded. The permeate stream was then discarded until the next desired precipitate concentration was achieved, after which the permeate stream was again recycled into the feed reservoir. This set of experiments were performed to investigate the impact of precipitate concentration on the permeate flux. A similar procedure was followed during the total recycle TFF experiments with the ELP-Z precipitates obtained during mAb elution.

2.2.3. Normal flow filtration (NFF)

NFF was employed for the recovery of the ELP-Z precipitates during mAb elution. All the NFF experiments were performed using the PendoTECH Filter Screening System (Princeton, NJ). 130 mL of 3.3 g/L mAb harvest was initially mixed with ELP-Z (in PBS) to achieve a 4:1 ELP-Z:mAb molar ratio. Na_2SO_4 (in PBS) was then added to obtain a 0.25 M final concentration to initiate ELP-Z-mAb precipitation. The precipitates were allowed to grow for 30 min, under the same mixing conditions as described in Section 2.2.2, followed by centrifugation at 4000 × *g* for 30 min. The supernatant containing the impurities was discarded and the ELP-Z-mAb precipitates were resolubilized in the elution buffer (50 mM citrate, pH 4). Na_2SO_4 (in the elution buffer) was then added to a 0.25 M final concentration to initiate ELP-Z precipitation. This resulted in ~200 mL of elution pool. The precipitates were mixed for 30 min and then transferred to a pressure controlled steel cylinder to perform NFF. 17.3 cm^2 NFF filters with 5, 1.2, 0.65 and 0.45/0.2 μm average effective pore size were employed for this study resulting in ~116 L/m^2 filter loading. All the NFF experiments were performed at a constant differential pressure (DP) of 5 psig and the membranes were pre-equilibrated with the precipitation buffer (50 mM citrate, 0.25 M Na_2SO_4, pH 4) before the experiment. During the filtration experiments, the mass of the collected permeate stream was recorded as a function of time and was later converted to volume (assuming a 1 kg/L density). The permeate stream after every filtration run was analyzed for turbidity using a portable 2100Q Turbidimeter (Hach, Loveland, Colorado) to determine the presence of transmitted ELP-Z precipitates. Formazin reference standards were used for calibration of the instrument. The ELP-Z precipitates were recovered from the NFF membrane by recirculation of PBS multiple times through the membrane which was then analyzed by RPLC to determine the ELP-Z recovery.

2.2.4. Laser scanning confocal microscopy

A Zeiss LSM 510 laser scanning confocal microscope (Carl Zeiss MicroImaging, LLC, Thornwood, New York, NY, USA) was used for imaging the ELP-Z and ELP-Z-mAb precipitates. Both the ELP-Z and the ELP-Z-mAb precipitates were imaged using bright field imaging. The precipitate feeds were transferred on to a cover glass using a pipette at specific time intervals (5, 10 or 30 min) after initiating precipitation and the imaging was performed using a 405 nm Argon laser with either Plan-Neofluar 25x/0.8 Imm corr DIC or alpha Plan-Fluar 100x/1.45 oil objectives.

2.3. Analytical methods

2.3.1. Reversed phase liquid chromatography (RPLC)

RPLC was used to analyze the mixtures (supernatants and resolubilized precipitates) from the mAb affinity precipitation experiments and to quantify the ELP-Z and mAb recoveries. RPLC was carried out using a C4 column (4.6 mm × 50 mm) as described previously (Sheth et al., 2014).

2.3.2. Size exclusion chromatography (SEC)

SEC was employed to analyze the final supernatants after the mAb elution screens and to determine the mAb aggregate content as described previously (Sheth et al., 2014).

2.3.3. Analytical protein A chromatography

Analytical Protein A chromatography was carried out using a POROS® A 20 μm column as described previously (Sheth et al., 2014) to determine mAb yield/recoveries during the affinity precipitation processes when the mAb harvest feed was employed.

2.3.4. ELISA host cell protein analysis

A 3rd generation generic ELISA kit from Cygnus Technologies was employed to quantify CHO host cell protein (HCP) levels in various samples as described previously (Sheth et al., 2014). The assay quantification limit was 1 ng/mL.

2.3.5. DNA analysis

The residual DNA content in the mAb elution pools was determined using a quantitative PCR (qPCR) method developed in house at BMS. 2 qPCR measurements were performed for every sample and the DNA assay variations were ~5%. The quantification limit was 0.2 pg/mL.

3. Results and discussion

The ELP-Z based mAb affinity precipitation process is carried out sequentially using the following steps: (1) the binding of ELP-Z to the mAb followed by precipitation of the ELP-Z-mAb complex; and (2) re-solubilization of the ELP-Z-mAb precipitates in the elution buffer followed by precipitation of the ELP-Z to recover the purified mAb in the final supernatant. The efficiency of the precipitate recovery steps and the corresponding throughputs are major determinants of the scalability of a precipitation based approach. While

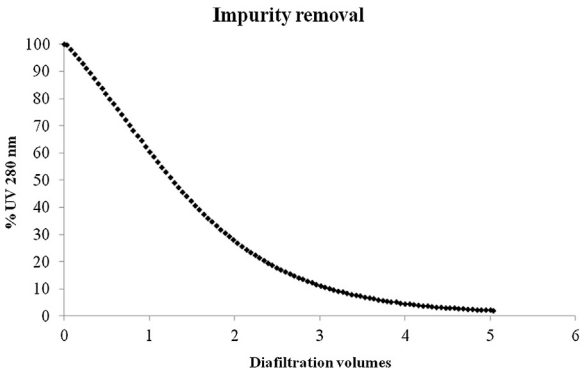

Fig. 1. UV absorbance trace of the permeate stream during diafiltration of the ELP-Z-mAb precipitates.

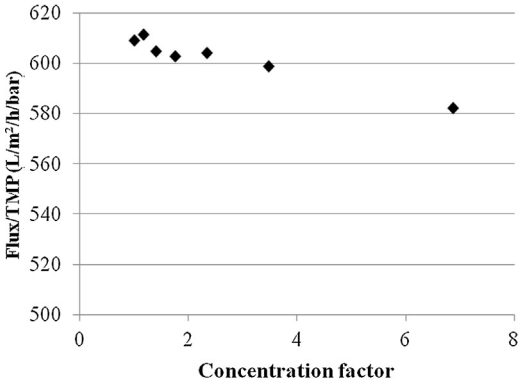

Fig. 2. Permeate flux during total recycle experiment of ELP-Z-mAb precipitates at different slurry concentrations.

the first step of this affinity precipitation process requires recovery of the ELP-Z-mAb precipitates, the second step requires the recovery of both the ELP-Z precipitates and the mAb supernatant.

3.1. Tangential flow filtration (TFF) for ELP-Z-mAb precipitate recovery

TFF was employed for the recovery of the ELP-Z-mAb precipitates formed during the first step of the affinity precipitation process. The objective of this unit operation was to first concentrate the ELP-Z-mAb precipitates and to then use diafiltration for the removal of impurities. Previous work in our lab has shown that when this affinity precipitation process is carried out at room temperature (22 °C), the process results in high mAb yields and purity with low aggregation of the mAb. Accordingly, all the evaluations in the current work were performed at room temperature.

The ELP-Z-mAb precipitates had a broad particle size distribution with an average particle diameter of ~15 μm (based on %volume) with some "fines" present in the sub-micron size range as determined by laser light scattering (data not shown). Accordingly, a hydrophilized PVDF membrane with a 0.1 μm average effective pore size was employed for the initial TFF studies to assure minimal loss of the precipitates. A 4:1 ELP-Z:mAb molar ratio was employed for mAb binding which had been previously shown to recover >99% of the mAb from the harvest feed (Sheth et al., 2014). As described in Section 2.2.2, the precipitation was initiated by addition of Na_2SO_4 to achieve a 0.25 M final concentration in the feed and a 0.25 M Na_2SO_4 in PBS buffer was employed for the subsequent diafiltration steps.

The ELP-Z-mAb precipitate feed was concentrated two times before initiating the diafiltration. In-line permeate UV absorbance at 280 nm was monitored during diafiltration and the resulting profile is given in Fig. 1. Since the majority of the mAb was bound to the ELP-Z (as verified by analytical Protein A chromatography), the absorbance trace was indicative of the presence of impurities in the permeate stream. As can be seen in the figure, as the supernatant was progressively replaced by the pure precipitation buffer during diafiltration, the absorbance of the permeate stream was continuously reduced. This resulted in greater than 98% reduction of the permeate UV absorbance in 5 diavolumes, indicating that most of the soluble impurities were removed during diafiltration (note: this was also verified by HCP and DNA analysis shown in Table 1). It was also observed that the permeate stream was clear (turbidity 1 NTU), which indicated that most of the precipitates were retained on the membrane. These results indicate that TFF was successful in achieving good retention of the ELP-Z-mAb precipitates and high diafiltration efficiency in removing soluble host cell and media impurities.

An important consideration in determining the scalability of this TFF step was the volumetric throughputs that could be achieved. Thus, it was of interest to determine the permeate flux during the TFF process. In order to minimize buffer consumption during the process, it would be desirable to concentrate the precipitate suspension to low volumes and to then perform the diafiltration. However, for a TFF unit operation, the permeate flux is a function of retained solute content at given process parameters and concentrating the slurry may lead to reduction in the permeate flux and long diafiltration times.

Accordingly, TFF in total recycle mode of operation was employed to determine the permeate flux as a function of ELP-Z-mAb feed/precipitate concentration. The precipitate concentration factor was determined assuming 100% precipitate retention. As described in Section 2.2.2, the system was allowed to reach a stable permeate flux at a given slurry concentration and the flux was recorded. A certain volume of permeate was then collected to increase the slurry concentration and the system was then switched back into total recycle mode to determine the permeate flux. This procedure was repeated and the results are presented in Fig. 2 which shows the normalized permeate flux ($L/m^2/h/bar$) as a function of the concentration factor of the ELP-Z-mAb slurry in the feed. As can be seen in the figure, the permeate flux was high (~610 $L/m^2/h/bar$) at the initial feed condition. Although flux appeared to be a function of solute content, a very high flux was maintained (~580 $L/m^2/h/bar$) even at a concentration factor of 7. This suggests that high feed volume reductions can be achieved before the diafiltration process without any significant reduction in the permeate flux, thus enabling low buffer consumption and rapid overall processing times. Taken together, the results shown in Figs. 1 and 2 suggest that the initial ELP-Z-mAb precipitate recovery step can be effectively performed using a TFF unit operation which is known to be readily scalable.

3.2. TFF for the recovery of ELP-Z precipitates

Precipitates containing the ELP-Z-mAb complex recovered during the first step of the process were then suspended in a 50 mM citrate, pH 4 elution buffer which resulted in the dissociation of the ELP-Z-mAb complex as well as resolublization of the precipitates. Na_2SO_4 was then added to obtain a final concentration of 0.25 M to precipitate the ELP-Z, leaving the dissociated mAb in the supernatant. TFF with the same membrane cassette and process parameters used in the initial recovery step described above was then employed to retain the ELP-Z precipitates on the membrane surface and to recover the mAb product in the permeate pool. Diafiltration was then performed using the precipitation buffer to

Table 1
Analysis of the process streams during the TFF unit operations.

Sample	mAb (Pro A)	ELP-Z (RPLC)	Observation	HCP (ppm)	DNA (ppb)
Permeate step 1	<0.5%	<DL	Clear liquid	ND	ND
mAb elution pool (permeate Step 2)	94.1%	<DL	Clear liquid	4900	10,125
ELP-Z resolubilized after elution	2–3%	87.22%	Slightly turbid	2839	7300

DL-Detection limit; ND-Not determined.

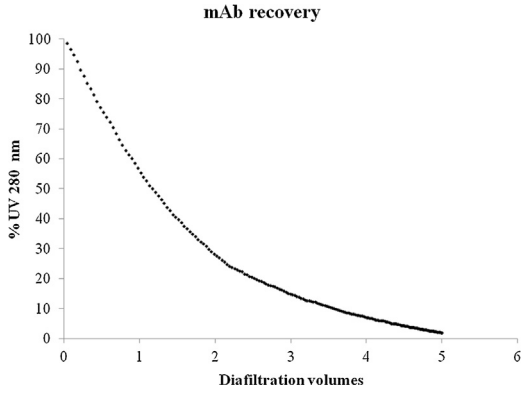

Fig. 3. UV absorbance trace of the permeate stream during diafiltration of the ELP-Z precipitates.

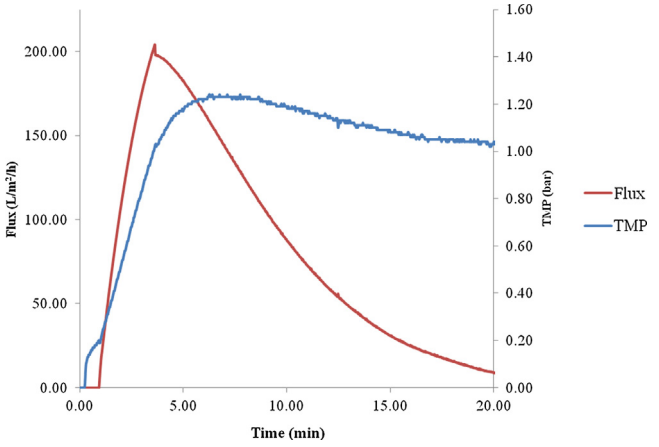

Fig. 4. Permeate flux as a function of time during the total recycle of the initial ELP-Z precipitate slurry.

increase the yield of recovered mAb product from the ELP-Z precipitates.

Fig. 3 shows the in-line 280 nm UV absorbance trace of the permeate stream during the diafiltration step. The UV absorbance in this experiment was indicative primarily of the presence of eluted mAb product in the permeate stream. As can be seen in the figure, the permeate stream UV absorbance was progressively reduced as the diafiltration buffer replaced the mAb supernatant in the retentate reservoir. This resulted in ~98.2% reduction in the permeate UV absorbance in 5 diavolumes indicating that most of the eluted mAb was recovered in the permeate stream (note: this was verified by analytical Protein A chromatography as discussed below in Table). In addition, the permeate stream was also clear (turbidity: 1 NTU), which indicated that the ELP-Z precipitates were efficiently retained on the membrane.

Table presents quantitative results for the mAb and ELP-Z concentrations in the permeate pools from both the ELP-Z-mAb binding and the mAb elution steps of the process using TFF. The mAb and ELP-Z concentrations were determined by protein A and RPLC, respectively, as described in the methods section. As can be seen in the table, the permeate stream during step 1 (ELP-Z-mAb binding followed by precipitation) contained <0.5% mAb and no detectable ELP-Z which confirms that the UV absorbance of the permeate stream was primarily due to the impurities. The analysis of the permeate stream during step 2 (mAb elution) showed a 94.1% mAb yield and no detectable ELP-Z. The mAb elution pool after step 2 contained ~0.45 g/L mAb. The low final mAb concentrations occurred due to the 5 diafiltration volumes employed for mAb recovery. This however can be mitigated by performing diafiltration at higher ELP-Z slurry concentrations. In addition, the ELP-Z-mAb precipitates from the first step can also be resolubilized in a lower volume of the elution buffer to achieve significantly higher mAb concentrations.

The mAb elution pool was also analyzed for the presence of HCP and DNA impurities. The mAb harvest feed contained ~3×10^5 ppm HCP and ~3.6×10^6 ppb DNA. The mAb elution pool results in Table suggest that while the process resulted in good HCP and DNA clearance, these impurity levels were higher than those obtained in previously published batch studies (Sheth et al., 2014) which resulted in ~1500 ppm HCP and ~100 ppb DNA in the elution pool. This is likely due to the diafiltration operation employed during the first TFF. The results in Fig. 1 showed that for 5 diavolumes, the UV absorbance of the permeate stream had not completely reached baseline indicating that the soluble impurities were not completely removed. Employing higher diafiltration volumes during this step would reduce the impurity carryover to the final elution pool. Employing higher diafiltration volumes would also increase the buffer consumption and processing times. However, this problem can be mitigated by performing diafiltration at higher precipitate concentrations.

The ELP-Z precipitates retained on the membrane after the second precipitation step were resolubilized using PBS buffer and analyzed for ELP-Z recovery and leftover mAb and impurity content. As can be seen in Table 1, the resolubilized ELP-Z contained low levels of residual mAb, HCP and DNA impurities which were consistent with previously published batch results (Sheth et al., 2014). Interestingly, ELP-Z recovery was only 87% for the entire process which was lower than the batch results (~93%). This could be due to non-specific adsorption of ELP-Z onto the membrane surface or system components. Another observation that was made was that the resolubilized ELP-Z pool was slightly turbid, which could be due to the formation of irreversible precipitates by the ELP-Z, mAb and/or some of the impurities.

Permeate flux behavior during step 2 (mAb elution) of the process was then evaluated by performing a total recycle experiment as described in Section 2.2.2. Fig. 4 shows the permeate flux as a function of time during this analysis. As can be seen in the figure, while the flux initially increased with the transmembrane pressure, it then exhibited a rapid decline to negligible flux in 20 min, at which point the experiment was stopped. This suggests that in contrast to the results from the first step of the process, the ELP-Z precipitates from the second step severely fouled the TFF membrane. These ELP-Z precipitates (2–5 μm by confocal microscopy as shown in Fig. 5) were much larger than the 0.1 μm membrane pore size and were thus unlikely to cause pore constriction due to internal pore-surface fouling. Another explanation for this flux reduction could be due to accumulation of these precipitates on to the membrane surface. Interestingly, the significant flux reduction

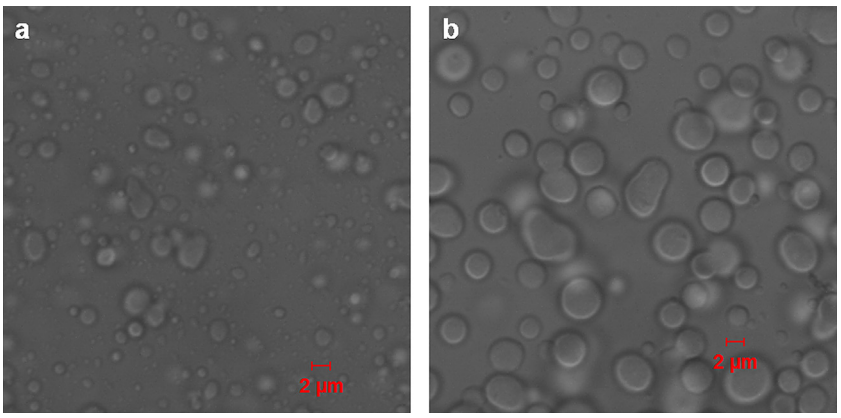

Fig. 5. ELP-Z precipitates bright field image. (a) ELP-Z precipitates 5 min after initiating precipitation and (b) ELP-Z precipitates 30 min after initiating precipitation.

shown in Fig. 4 occurred at a relatively high volumetric cross-flow rate (960 L/m^2/h) in the TFF system, which further indicates the irreversible nature of the membrane fouling.

These results may also explain the lower ELP-Z recovery from the TFF membrane in step 2 shown in Table 1. Thus, while the results shown in Fig. 3 demonstrated that the feed to step 2 could be processed before the flux decay occurred at the given loading, the results in Fig. 4 clearly indicate that this approach may not be applicable for processing higher feed loading typical of a commercial scale process.

The results shown in Figs. 2 and 4 demonstrate that the precipitates formed during the two stages of the affinity precipitation process behaved quite differently during the TFF steps. One possible reason why the ELP-Z-mAb precipitates in the first step did not foul the TFF membrane could be that these precipitates contained almost equal amounts of the hydrophobic ELP-Z and the relatively hydrophilic mAb. This is in contrast to the ELP-Z precipitates in step 2 which consisted solely of the hydrophobic ELP-Z. We hypothesized that this difference in the net hydrophobicity of the precipitates could alter their propensity to foul the membrane.

3.3. Characterization of ELP-Z and ELP-Z-mAb precipitates

In order to shed some light on the significant differences in the flux behaviors of the two precipitates, confocal microscopy was carried out. ELP precipitates have been shown to grow in size via a coalescence mechanism (Osborne et al., 2008; Zhang et al., 2003) where the particles fuse together due to higher interfacial tension between the particle surface and the surrounding medium (solvent). Importantly, these precipitates retain a spherical geometry and a homogenous texture after coalescence. It should also be noted that the ELP is fused to the Z domain in the current study, which may alter the precipitation behavior.

Fig. 5 shows the bright field image of ELP-Z precipitates from step 2 at 5 and 30 min after initiating the precipitation. As can be seen in Fig. 5a, at 5 min the ELP-Z precipitates had a particle size distribution ranging from submicron to approximately 3 μm. At 30 min, the ELP-Z precipitates had particle sizes ranging from approximately 2–5 μm (Fig. 5b). Importantly, most of the submicron particles observed in Fig. 5a, were not present in Fig. 5b. This indicates that the net ELP-Z size increased over time, which is to be expected during precipitation. Fig. 5 also shows that while most of the particles had a spherical geometry, some particles possessed oblate geometry which was indicative of the ongoing coalescence between two or more ELP-Z particles. This coalescence mechanism also supports the hypothesis that the ELP-Z precipitates from step 2 were quite hydrophobic in nature and that they tended to adhere to surfaces in the TFF system.

The ELP-Z-mAb precipitates from step 1 were also examined using confocal microscopy. Fig. 6 shows the confocal image of the ELP-Z-mAb precipitates that occurred at a 4:1 ELP:mAb molar ratio at two magnifications. As can be seen from Fig. 6a, the ELP-Z-mAb precipitates formed large agglomerates which were much larger than the ELP-Z precipitates from step 2. While the images in Fig. 6 were taken 10 min after initiating the precipitation. Large precipitates could also be readily distinguished within minutes of precipitation, even by visual inspection. These results indicate that the kinetics of ELP-Z-mAb precipitation was quite fast. Further examination of an isolated ELP-Z-mAb precipitate at a higher magnification (Fig. 6b), suggested that the ELP-Z-mAb precipitates were non-homogenous in nature in contrast to the ELP-Z precipitates from step 2. Importantly, these precipitates seemed to be formed by the assembly of multiple sub-micron sized precipitates.

Clearly, these confocal results suggested that the ELP-Z and ELP-Z-mAb precipitates were qualitatively quite different. While the precipitation kinetics under continuous mixing conditions employed during actual processes could be different, the differences in the morphologies and the nature of the precipitates would still be expected to play an important role.

3.4. Normal flow filtration (NFF) for ELP-Z precipitate recovery

Due to the limited success of the TFF unit operation for the recovery of the ELP-Z precipitates during the second step of the affinity precipitation process, an alternative disposable normal flow filtration (NFF) strategy was evaluated. Fig. 7 shows the staged normal flow filtration (NFF) train scheme that was initially examined for the ELP-Z precipitate recovery. The filter train started with a large pore size filter (5 μm) and ended with a relatively small filter (0.45/0.2 μm). The objective of this NFF train was to evaluate the ELP-Z precipitate recovery and throughput at each stage of the filtration and to design a NFF unit operation that could maintain high throughput during the ELP-Z precipitate recovery step. In this experiment, the presence of ELP-Z in the filtered mAb product pool was determined using turbidity measurements and quantified by RPLC analysis. The permeate flux was also monitored to determine the volumetric throughput of this unit operation.

Table 2 presents the filter train analysis of ELP-Z precipitates during the mAb elution step. All the NFF experiments were performed at a constant differential pressure (DP) of 5 psig. The initial ELP-Z precipitate feed turbidity was ~500 NTU. As can be seen in Table 2, the 5 μm filter resulted in significant reduction in the turbidity for the ELP-Z feed. RPLC analysis indicated that less than 0.5% ELP-Z sieved through the filter, which was quite low. The subsequent 1.2 μm filter was able to retain the remaining ELP-Z precipitates with the ELP-Z content in the permeate being below

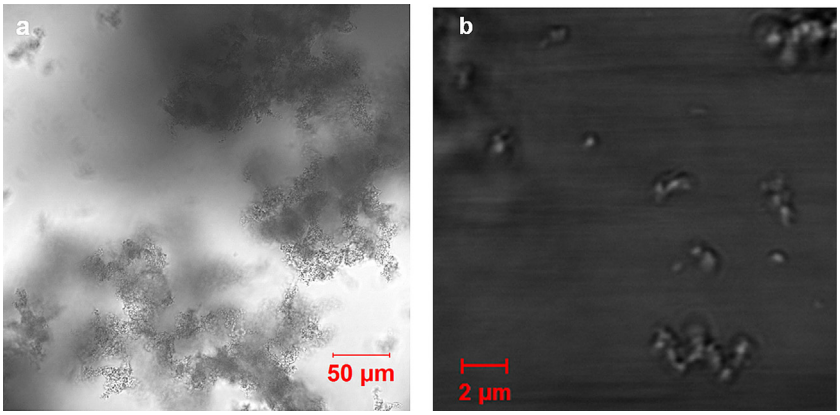

Fig. 6. ELP-Z-mAb complex precipitates bright field image for 4:1 ELP-Z:mAb molar ratio after 10 min. (a) Scale bar 50 μm and (b) higher resolution image, scale bar 2 μm.

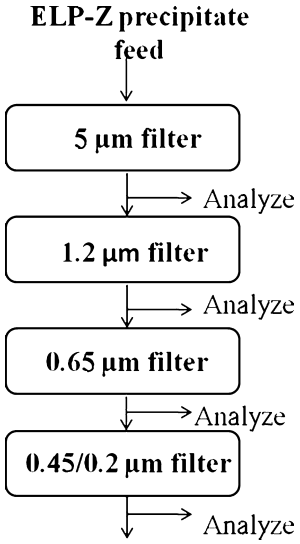

Fig. 7. Normal flow filtration (NFF) train scheme employed for the recovery of ELP-Z precipitates during mAb elution.

Table 2
Analysis of the permeate streams during the ELP-Z precipitate recovery using the staged normal flow filtration scheme.

NFF membrane	Turbidity (NTU)	mAb yield (%)
5 μm	5 (0.4% ELPZ)	94.2
1.2 μm	2	93.3
0.65 μm	1	90.7
0.45/0.2 μm	1	89.6

the RPLC assay detection limit. Finally, the 0.65 and 0.45/0.2 μm filters provided a clear permeate pool (note: a turbidity of 1 NTU corresponds to a clear solution). These results suggest that the 5 μm filter was able to retain most of the ELP-Z precipitates with the subsequent filters removed the remaining ELP-Z. The yield of the eluted mAb product was also determined in the permeate pools from each filtration step which included all previous steps in the process. As can be seen in Table 2, there was a minor reduction in the overall mAb yields after each step which could be due to non-specific interactions of the mAb with the membrane material.

Since the particle/precipitate content in the permeate pool from 5 μm filter was low, a simplified NFF train consisting of a 5 μm followed by a 0.45/0.2 μm filter was evaluated. The 0.45/0.2 μm filter was chosen here since most process streams are sterile filtered between downstream processing steps for bioburden control. Table 3 shows the results for this NFF train. The 5 μm filter again resulted in high levels of precipitate recovery. The 0.45/0.2 μm was able to retain all the remaining ELP-Z precipitates and provided a clear permeate stream. Importantly, as can be seen in the Table, higher overall mAb yield was obtained using this simplified process. In addition, low levels of HCP and DNA impurities were present in the final mAb elution pool. mAb aggregate content in the elution pool was shown to be comparable to the harvest feed (~4% by SEC).

Clearly, while the removal of the ELP-Z precipitates from the final mAb product was critical, it was also important to examine the recovery of the ELP-Z from the filters. Accordingly, the ability to recover ELP-Z precipitates retained on the 5 μm filter using a resolublizing buffer (cold PBS) was evaluated. By recirculating the buffer through the filter, ~96% overall ELP-Z recovery was attained. This may have important implications for reusing the ELP-Z for processing multiple feed lots.

It was also of interest to examine the permeate fluxes obtained in this NFF process. As can be seen in Fig. 8a, the very high flux at the beginning of the 5 um filtration step, was seen to reduce with increasing time to a final stabile value of ~500 L/m^2/h, which was still relatively high. This flux behavior is typical of a conventional normal flow/dead end filtration process where the flux is initially governed by the membrane pore size and later governed by the precipitate cake that forms on the filter membrane.

The permeate flux during the final 0.45/0.2 μm filtration was also examined (Fig. 8b). Since the feed to this filter was the permeate stream from the 5 μm filtration, the particle/precipitate load was relatively low. Accordingly, high permeate flux was obtained throughout the run starting at ~3000 LMH and ending at ~2400 LMH. The results shown in Figs. 8a and b clearly suggest that the 5 μm filtration was the rate determining step for the fluxes obtained during the ELP-Z precipitate recovery process using this scheme. Nevertheless, this simple dead end filtration scheme was

Table 3
Analysis of the permeate streams for the 5 μm and 0.45/0.2 μm filter combination during the final ELP-Z precipitate recovery.

NFF membrane	Turbidity (NTU)	mAb Yield (%)	HCP (ppm)	DNA (ppb)	HMW (%)
5 μm	5	96.9	ND	ND	ND
0.45/0.2 μm	1	95.6	2596	400	4.1

ND-Not determined.

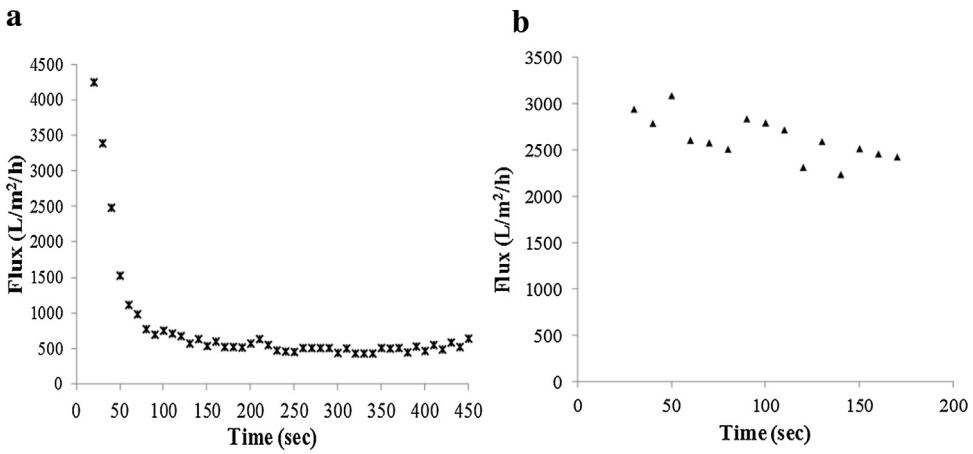

Fig. 8. Permeate flux during ELP-Z precipitate recovery using NFF. (a) Permeate flux during the 5 μm filtration of the ELP-Z precipitate feed and (b) Permeate flux during the 0.45/0.2 μm filtration of the permeate stream from the 5 μm filtration step.

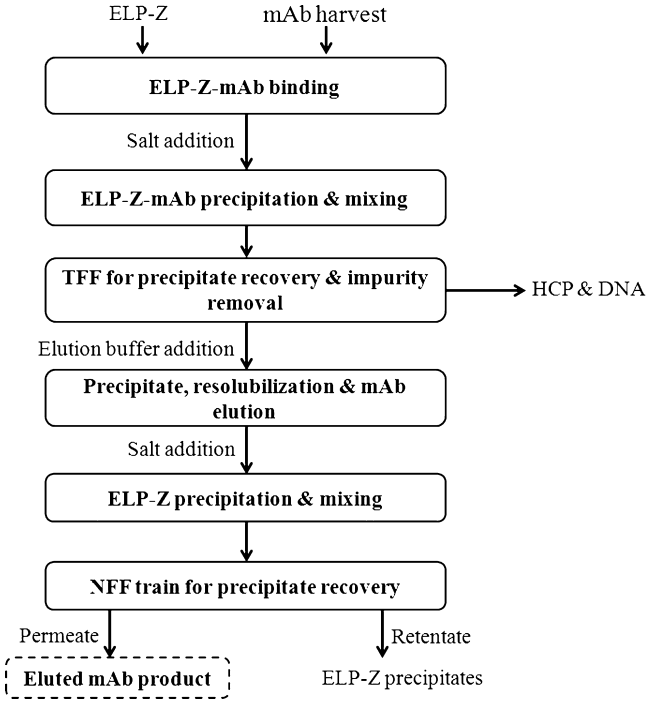

Fig. 9. A Schematic of the proposed ELP-Z based mAb affinity precipitation process for scale-up.

very successful in recovering the ELP-Z precipitates at relatively high volumetric throughputs.

The results presented in this paper suggest that a combination of TFF and NFF can be readily employed for the recovery of precipitates during the mAb affinity precipitation process at large scale. Fig. 9 represents a schematic of the proposed sequential batch process.

4. Conclusions

In this paper, a proof of concept ELP-Z based mAb affinity precipitation process was developed using scaled down filtration techniques. Tangential flow filtration (TFF) was initially examined for the recovery of ELP-Z-mAb precipitates formed during the mAb binding step and the ELP-Z precipitates created during the mAb elution step. Total recycle TFF experiments were employed to determine permeate fluxes as a function of the precipitate concentration for both stages of the process. While the ELP-Z-mAb precipitate recovery step was scalable with high permeate flux (550–600 L/m^2/h/bar), the ELP-Z precipitates resulted in severe fouling of the TFF membrane causing rapid flux decay. Confocal microscopy analysis of the ELP-Z-mAb and ELP-Z precipitates suggested that these precipitates were qualitatively quite different. While the ELP-Z precipitates were "sticky", homogenously spherical and grew by a coalescence mechanism; the ELP-Z-mAb precipitates were particulate in nature, non-homogenous and appeared to grow via agglomeration of smaller sub-micron sized units. In addition, the ELP-Z-mAb precipitation kinetics was quite fast as compared to ELP-Z kinetics. An alternative filtration approach was then developed for the second step. Using normal flow filtration with a combination of 5 μm and a 0.45/0.2 μm filters, the ELP-Z precipitates were removed from the final mAb product solution at high volumetric throughputs. Further, high ELP-Z recovery (96%) was obtained after resolubilization from the filter, indicating that the ELP-Z can potentially be reused multiple times. This proof of concept study demonstrates that the ELP-Z affinity precipitation process which was previously demonstrated using small scale batch studies (Sheth et al., 2014), can be readily scaled up using conventional membrane processing. Clearly, it will be necessary in actual applications to validate the removal of any residual ELP-Z by subsequent polishing steps, however, it is expected that this can be readily achieved using standard polishing chromatographic operations.

Acknowledgements

The authors would like to acknowledge Dr. Rieble Siegfried, Dr. Jia Liu, Dr. Jongchan Lee and Dr. Chao Huang for their insightful comments and discussion. The authors also acknowledge the Biologics Analytical Development & Testing group at Bristol-Myers Squibb for performing DNA analysis. This work was supported by National Science Foundation Grant CBET 0853948.

References

Banki, M.R., Feng, L., Wood, D.W., 2005. Simple bioseparations using self-cleaving elastin-like polypeptide tags. Nat. Methods 2, 4.

Belfort, G., Davis, R.H., Zydney, A.L., 1994. The behavior of suspensions and macromolecular solutions in crossflow microfiltration. J. Membr. Sci. 96, 1–58.

Bentham, A.C., Ireton, M.J., Hoare, M., Dunnill, P., 1988. Protein precipitate recovery using microporous membranes. Biotechnol. Bioeng. 31, 984–994.

Boychyn, M., Yim, S.S.S., Ayazi Shamlou, P., Bulmer, M., More, J., Hoare, M., 2001. Characterization of flow intensity in continuous centrifuges for the development of laboratory mimics. Chem. Eng. Sci. 56, 4759–4770.

Boychyn, M., Yim, S.S.S., Bulmer, M., More, J., Bracewell, D.G., Hoare, M., 2004. Performance prediction of industrial centrifuges using scale-down models. Bioprocess Biosyst. Eng. 26, 385–391.

Cho, Y., Zhang, Y., Christensen, T., Sagle, L.B., Chilkoti, A., Cremer, P.S., 2008. Effects of Hofmeister anions on the phase transition temperature of elastin-like polypeptides. J. Phys. Chem. B 112, 13765–13771.
Devereux, N., Hoare, M., 1986. Membrane separation of protein precipitates: studies with cross flow in hollow fibers. Biotechnol. Bioeng. 28, 422–431.
Fassina, G., 2001. Affinity Chromatography. eLS. John Wiley & Sons, Ltd., Chichester.
Ge, X., Trabbic-Carlson, K., Chilkoti, A., Filipe, C.D.M., 2006. Purification of an elastin-like fusion protein by microfiltration. Biotechnol. Bioeng. 95, 424–432.
Ge, X., Yang, D.S.C., Trabbic-Carlson, K., Kim, B., Chilkoti, A., Filipe, C.D.M., 2005. Self-cleavable stimulus responsive tags for protein purification without chromatography. J. Am. Chem. Soc. 127, 11228–11229.
Hilbrig, F., Freitag, R., 2003. Protein purification by affinity precipitation. J. Chromatogr. B 790, 79–90.
Hoare, M., Narendranathan, T.J., Flint, J.R., Heywood-Waddington, D., Bell, D.J., Dunnill, P., 1982. Disruption of protein precipitates during shear in Couette flow and in pumps. Ind. Eng. Chem. Fundam. 21, 402–406.
Hober, S., Nord, K., Linhult, M., 2007. Protein A chromatography for antibody purification. J. Chromatogr. B 848, 40–47.
Huse, K., Böhme, H.-J., Scholz, G.H., 2002. Purification of antibodies by affinity chromatography. J. Biochem. Biophys. Methods 51, 217–231.
Kim, J.-Y., O'Malley, S., Mulchandani, A., Chen, W., 2005. Genetically engineered elastin–protein A fusion as a universal platform for homogeneous, phase-separation immunoassay. Anal. Chem. 77, 2318–2322.
Madan, B., Chaudhary, G., Cramer, S.M., Chen, W., 2013. ELP-z and ELP-zz capturing scaffolds for the purification of immunoglobulins by affinity precipitation. J. Biotechnol. 163, 10–16.
Meyer, D.E., Chilkoti, A., 1999. Purification of recombinant proteins by fusion with thermally-responsive polypeptides. Nat. Biotechnol. 17, 4.
Meyer, D.E., Chilkoti, A., 2004. Quantification of the effects of chain length and concentration on the thermal behavior of elastin-like polypeptides. Biomacromolecules 5, 846–851.
Neal, G., Christie, J., Keshavarz-Moore, E., Shamlou, P.A., 2003. Ultra scale-down approach for the prediction of full-scale recovery of ovine polyclonal immunoglobulins used in the manufacture of snake venom-specific Fab fragment. Biotechnol. Bioeng. 81, 149–157.
Osborne, J.L., Farmer, R., Woodhouse, K.A., 2008. Self-assembled elastin-like polypeptide particles. Acta Biomater. 4, 49–57.
Sheth, R.D., Jin, M., Bhut, B.V., Li, Z., Chen, W., Cramer, S.M., 2014. Affinity precipitation of a monoclonal antibody from an industrial harvest feedstock using an ELP-Z stimuli responsive biopolymer. Biotechnol. Bioeng. 111, 1595–1603.
Sheth, R.D., Madan, B., Chen, W., Cramer, S.M., 2013. High-throughput screening for the development of a monoclonal antibody affinity precipitation step using ELP-z stimuli responsive biopolymers. Biotechnol. Bioeng. 110, 2664–2676.
Stiborova, H., Kostal, J., Mulchandani, A., Chen, W., 2003. One-step metal-affinity purification of histidine-tagged proteins by temperature-triggered precipitation. Biotechnol. Bioeng. 82, 605–611.
Sun, X.-L., Haller, C.A., Wu Conticello, V.P., Chaikof, E.L., 2005. One-pot glyco-affinity precipitation purification for enhanced proteomics: the flexible alignment of solution-phase capture/release and solid-phase separation. J. Proteome Res. 4, 2355–2359.
Urry, D.W., 1997. Physical chemistry of biological free energy transduction as demonstrated by elastic protein-based polymers. J. Phys. Chem. B 101, 11007–11028.
Venkiteshwaran, A., Heider, P., Teysseyre, L., Belfort, G., 2008. Selective precipitation-assisted recovery of immunoglobulins from bovine serum using controlled-fouling crossflow membrane microfiltration. Biotechnol. Bioeng. 101, 957–966.
Zhang, Y., Mao, H., Cremer, P.S., 2003. Probing the mechanism of aqueous two-phase system formation for α-elastin on-chip. J. Am. Chem. Soc. 125, 15630–15635.